International Journal of Heat and Mass Transfer 52 (2009) 4862–4872

Contents lists available at ScienceDirect

International Journal of Heat and Mass Transfer

journal homepage: www.elsevier.com/locate/ijhmt

A building corner model for hygrothermal performance and mould growth risk analyses

Gerson Henrique dos Santos [a,*], Nathan Mendes [a], Paulo Cesar Philippi [b]

[a] Thermal Systems Laboratory, Department of Mechanical Engineering, Pontifícia Universidade Católica do Paraná – PUCPR, R. Imaculada Conceição, 1155, Curitiba-PR 80.215-901, Brazil

[b] Laboratory of Porous Media and Thermophysical Properties, Department of Mechanical Engineering, Federal University of Santa Catarina, Florianópolis, CEP 88040-900, Brazil

ARTICLE INFO

Article history:
Received 3 November 2008
Received in revised form 2 May 2009
Accepted 2 May 2009

Keywords:
Coupled heat
Air and moisture transfer
Mould growth risk
Building corner simulation

ABSTRACT

Combined multidimensional analysis of heat, air and moisture transport through porous building elements is barely explored in the literature due to many difficulties such as modeling complexity, computer run time, numerical convergence and highly moisture-dependent properties. In this way, a mathematical model considering a combined two-dimensional heat, air and moisture transport through unsaturated building upper corners is presented. In order to improve the discretized model numerical stability, the algebraic equations are simultaneously solved for the three driving potentials: temperature, vapor pressure and moist air pressure gradients. In the results section, the convective effects caused by air stagnation are analyzed in terms of heat flux and mould growth risk for different boundary conditions, showing the importance of a detailed hygrothermal analysis – which is normally disregarded by simulation tools – for accurately predicting building energy consumption, indoor air quality, thermal comfort or mould growth risk.

1. Introduction

Residential, commercial and public buildings are greatly responsible for the total consumption of electricity, in a worldwide context. Only considering Brazil, they are responsible for at least 45% [1], which progressively motivates energy conservation studies for promoting building energy efficiency. In this context, many computer simulation tools have been developed [2] to evaluate energy performance of buildings from the early-stage sketches to the complex existing buildings. Nevertheless, building energy simulation tools do not consider the multidimensionality nature of heat and mass transfer through building envelopes.

When the multidimensional effect is considered, thermal bridges may play an important role. Thermal bridges appear in places where the envelope changes its geometry (ex: corners) or composition or both. Thermal bridge is used to define each part of the building envelope where, there is a local increase of heat flux density and a decrease or increase of internal surface temperatures. Beyond the thermal effect, the mass transport is also affected in the corner region and this fact is still barely explored in the literature.

The available literature is focused on the thermal effects. Brown and Wilson [3] analyzed the insulation effect with some examples and illustrated factors that influence the thermal performance of the thermal bridges. Hassid [4] proposed a correction to the one-directional heat transfer algorithms, to account for heat transfer across thermal bridges between parallel elements. In another work, Hassid [5] implemented into the ESP building energy simulation program this model and showed to be able to predict the order of magnitude of changes due to corner effects and thermal bridges. These effects were not negligible to the prediction of internal surface temperature.

Krarti [6] described an analytical, two-dimensional steady-state thermal analysis of insulated square corners. The results showed that, even thought corner heat loss is reduced with increasing insulation thermal resistance, the risk of moisture damage increases. Tang and Saluja [7] presented an analytical solution for the elliptic boundary value problem with irregular geometrical boundary region. The application of the solution was addressed to the physical problems of temperature distribution and heat flux within homogeneous corners of buildings.

Farkh [8] described the principles and method for the analysis of the bridges, presenting default values, calculated according to the French standards. These values were obtained using linear coefficients for different thermal bridge configurations. Olsen and Radisch [9] organized a report about thermal bridges in residential buildings in Denmark, describing the Danish building regulations and standards. This report cites that a Nordic study showed that the transmission loss is likely to increase by 10–50% when more correct calculations of thermal bridges are introduced and, in some

* Corresponding author. Tel.: +55 41 3271 1691.
E-mail addresses: gerson.santos@pucpr.br (G.H. dos Santos), nathan.mendes@pucpr.br (N. Mendes), philippi@lmpt.ufsc.br (P.C. Philippi).

0017-9310/$ - see front matter © 2009 Elsevier Ltd. All rights reserved.
doi:10.1016/j.ijheatmasstransfer.2009.05.026

Nomenclature

c_0	specific heat capacity of the dry material (J/kg K)
c_m	specific heat of the structure (J/kg K)
c_{pa}	specific heat capacity at constant pressure of the dry air (J/kg K)
c_{pl}	specific heat capacity of the water liquid (J/kg K)
c_{pv}	specific heat capacity at constant pressure of the vapor (J/kg K)
$\mathbf{g}$	gravity (m/s^2)
h	convective heat transfer coefficient (W/m^{2}K)
$\mathbf{j}$	density of moisture flow rate (kg/m^2 s)
$\mathbf{j_l}$	density of liquid flow rate (kg/m^2 s)
$\mathbf{j_v}$	density of vapor flow rate (kg/m^2 s)
$\mathbf{j_a}$	density of dry air flow rate (kg/m^2 s)
j	density of moisture flow rate (kg/m^2 s)
L	vaporization latent heat (J/kg)
K	liquid water permeability (s)
P_{suc}	suction pressure (Pa)
P_v	partial vapor pressure (Pa)
P_g	gas pressure (dry air pressure plus vapor pressure) (Pa)
q	heat flowing into structure (external) (W/m^2)
T	temperature (K)
w	moisture content (kg/m^3)

Greeks

α	absorptivity (–)
β_v	surface coefficient of water vapor transfer (s/m)
δ_v	vapor diffusive permeability (s)
ϕ	relative humidity (–)
k	absolute permeability (m^2)
k_{rg}	vapor relative permeability (–)
λ	thermal conductivity (W/mK)
μ_g	dynamic viscosity (Pa s)
ρ_a	density of dry air (kg/m^3)
ρ_l	liquid water density (kg/m^3)
ρ_v	vapor density (kg/m^3)
ρ_0	density of the dry material (kg/m^3)

cases, that difference can amount up to more than 60% of the total transmission losses, showing definitely how important thermal bridges are, especially for cold Nordic weathers.

Csoknyai [10] monitored the film coefficient value along the edges and at thermal bridges and showed that it differs from the overall standard design value and varies as a function of temperature and several further random effects. Kosny and Kossecka [11] showed that in most whole building thermal modeling computer programs such as DOE-2, BLAST and Energyplus, where simplified one-dimensional, parallel path model is used, the building load estimations may generate serious errors due to the thermal bridge effects.

Beyond the thermal effects, when surface temperatures decreases (cold climate), condensation may occur. This condensation can promote the germination and growth of mould on wall surfaces. On the other hand, in hot climates, mould growth can be influenced by stagnation air around the corner region.

Mould may damage surfaces, causing unpleasant 'musty' odors and health hazards from spores released by the moulds. Therefore, models for predicting the mould growth become an important tool for assuring the well-being of occupants.

However, just a few models can be found in the literature. Adan [12] describes the initial growth-lag, acceleration phase and log-growth phase of mould fungi. The *Time of Wetness* (TOW) (number of hours of high relative humidity, e.g., 80%, per day) is utilized to assess the transient evolution of the mould formation.

Clarke et al. [13] formulated six generic mould categories in terms of the combination of temperature and relative humidity for which mould growth would occur on building materials. However, the mould growth model is not transient.

Hukka and Viitannen [14] developed a model based on the relative humidity and temperature that allows determining the temporal development of the mould growth. However, this model has been especially developed for wood.

Moon and Augenbroe [15] suggested a "performance indicator" (PI) that expresses the mold growth risk in existing buildings as the causal effect of certain building parameters (physical state of the building, HVAC systems and layout, maintenance and cleaning operation).

As observed in the above mentioned works on thermal bridge, only thermal effects are verified in the corner region and an analysis of the internal convective heat transfer coefficient effect on the mould growth and hygrothermal performance is barely found in the literature.

Therefore, in order to analyze the effects of building hygrothermal envelope corners, a multidimensional model has been developed to calculate the coupled heat, air and moisture transfer through building envelopes. For ensuring numerical stability in the present model, the linearized set of equations has been obtained by using the finite-volume method and the MultiTriDiagonal-Matrix Algorithm [16] to solve a 2-D HAM model to describe the physical phenomena of heat, air and mass (HAM) transfer through porous building materials. The mould growth in the corner region has been analyzed through the model proposed by Clarke et al. [13]. Section 2 of this paper shows the mathematical model, while Section 3 presents the simulation procedure and Sections 4 and 5 the results and conclusions.

2. Mathematical model

The model for the porous media domain has been elaborated considering the differential governing equations for moisture, air and energy balances. The transient terms of each governing equation have been written in terms of the driving potentials to take more advantage of the MTDMA [16,17] solution algorithm.

2.1. Moisture transport

The moisture transport has been divided into liquid and vapor flows as shown in the below equation:

$$\mathbf{j} = \mathbf{j_l} + \mathbf{j_v}, \tag{1}$$

where $\mathbf{j}$ is the density of moisture flow rate (kg/m^2 s), $\mathbf{j_l}$ is the density of liquid flow rate (kg/m^2 s), and $\mathbf{j_v}$ is the density of vapor flow rate (kg/m^2 s).

The liquid transport calculation is based on the Darcy equation:

$$\mathbf{j_l} = K(\nabla P_{suc} - \rho_l \mathbf{g}), \tag{2}$$

where K is the liquid water permeability (s), P_{suc} is the suction pressure (Pa), ρ_l is the liquid water density (kg/m^3) and $\mathbf{g}$ is the gravity (m/s^2).

The capillary suction pressure can be written as a function of temperature and moisture content in the following form:

$$\nabla P_{suc} = \frac{\partial P_{suc}}{\partial T}\nabla T + \frac{\partial P_{suc}}{\partial P_v}\nabla P_v. \tag{3}$$

Similarly to the liquid flow, the vapor flow is calculated from the Fick equation considering effects of both vapor pressure and air pressure driving potentials:

$$\mathbf{j_v} = -\underbrace{\delta_v \nabla P_v}_{\text{vapor diffusion}} - \underbrace{\rho_v \frac{k k_{rg}}{\mu_g} \nabla P_g}_{\text{convective vapor transport}}, \tag{4}$$

where δ_v is the vapor diffusive permeability (s), P_v is the partial vapor pressure (Pa), ρ_v is the vapor density (kg/m^3), k is the absolute permeability (m^2), k_{rg} is the vapor relative permeability, μ_g is the dynamic viscosity (Pa s) and, P_g is the gas pressure.

The water mass conservation equation can be described as:

$$\frac{\partial w}{\partial t} = -\nabla \cdot \mathbf{j}, \tag{5}$$

where w is the moisture content (kg/m^3).

This moisture content conservation equation – Eq. (5) – can be written in terms of the three driving potentials as:

$$\frac{\partial w}{\partial \phi}\frac{\partial \phi}{\partial P_v}\frac{\partial P_v}{\partial t} + \frac{\partial w}{\partial \phi}\frac{\partial \phi}{\partial T}\frac{\partial T}{\partial t} = \nabla \cdot \left[-K \frac{\partial P_{suc}}{\partial T} \nabla T - \left(K \frac{\partial P_{suc}}{\partial P_v} - \delta_v \right) \nabla P_v + \rho_v \frac{k k_{rg}}{\mu_g} \nabla P_g + K \rho_l \mathbf{g} \right]. \tag{6}$$

2.2. Air transport

In the proposal model, the air transport is individually considered through the dry-air mass balance. In this way, the dry-air conservation equation can be expressed as:

$$\frac{\partial \rho_a}{\partial t} = -\nabla \cdot \mathbf{j_a}, \tag{7}$$

with the air flow calculated by the following expression:

$$\mathbf{j_a} = \underbrace{\delta_v \nabla P_v}_{\text{air diffusion}} - \underbrace{\rho_a \frac{k k_{rg}}{\mu_g} \nabla P_g}_{\text{air convection}}, \tag{8}$$

where ρ_a is the density of dry air (kg/m^3), $\mathbf{j_a}$ is the density of dry air flow rate (kg/m^2 s), and P_g is the gas pressure (dry air pressure plus vapor pressure) in Pa.

Therefore, the dry air transport can be described as a function of the partial gas and vapor pressure driving potentials so that the air balance can be written as:

$$\frac{\partial \rho_a}{\partial P_g}\frac{\partial P_g}{\partial t} + \frac{\partial \rho_a}{\partial P_v}\frac{\partial P_v}{\partial t} + \frac{\partial \rho_a}{\partial T}\frac{\partial T}{\partial t} = \nabla \cdot \left(-\delta_v \nabla P_v + \rho_a \frac{k k_{rg}}{\mu_g} \nabla P_g \right). \tag{9}$$

2.3. Heat transport

The transient energy balance including phase change is described as:

$$c_m \rho_0 \frac{\partial T}{\partial t} = -\nabla \cdot \mathbf{q} + S, \tag{10}$$

where c_m is the mean specific heat of the structure (J/kg K), ρ_0 is the dry-basis material density (kg/m^3), and S is the source term (W/m^3) due to phase change.

The heat flux can be attributed to both conductive and convective effects:

$$\mathbf{q} = \mathbf{q_{cond}} + \mathbf{q_{conv}}, \tag{11}$$

where

$$\mathbf{q_{cond}} = -\lambda \nabla T \tag{12}$$

and

$$\mathbf{q_{conv}} = \underbrace{\mathbf{j_l} c_{pl} T}_{\text{liquid flow}} + \underbrace{\mathbf{j_a} c_{pa} T}_{\text{dry air flow}} + \underbrace{\mathbf{j_v} c_{pv} T}_{\text{vapor flow}}, \tag{13}$$

where λ is the thermal conductivity (W/mK), c_{pa} is the dry air specific heat at constant pressure (J/kg K), c_{pl} is the water specific heat (J/kg K), and c_{pv} is the water vapor specific heat at constant pressure (J/kg K). The source term is calculated by means of the vaporization latent heat as:

$$S = -L(T) \nabla \cdot \mathbf{j_v}, \tag{14}$$

In this way, assuming a reference temperature of 0 °C, the energy conservation equation can be written in terms of the three driving potentials as:

$$c_m \rho_0 \frac{\partial T}{\partial t} = \nabla \cdot \begin{pmatrix} (\lambda - K \frac{\partial P_{suc}}{\partial T} c_{pl} T) \nabla T - \left(K \frac{\partial P_{suc}}{\partial P_v} c_{pl} T + \delta_v c_{pa} T - \delta_v c_{pv} T \right) \nabla P_v + \\ \left(\rho_a \frac{k k_{rg}}{\mu_g} c_{pa} T + \rho_v \frac{k k_{rg}}{\mu_g} c_{pv} T \right) \nabla P_g + K \rho_l c_{pl} T \mathbf{g} \end{pmatrix} - L(T) \nabla \cdot \mathbf{j_v} \tag{15}$$

2.4. Boundary conditions

In the dry-air conservation equation of the present model, gas pressure has been considered as a prescribed value – Dirichlet condition – at the envelope surface:

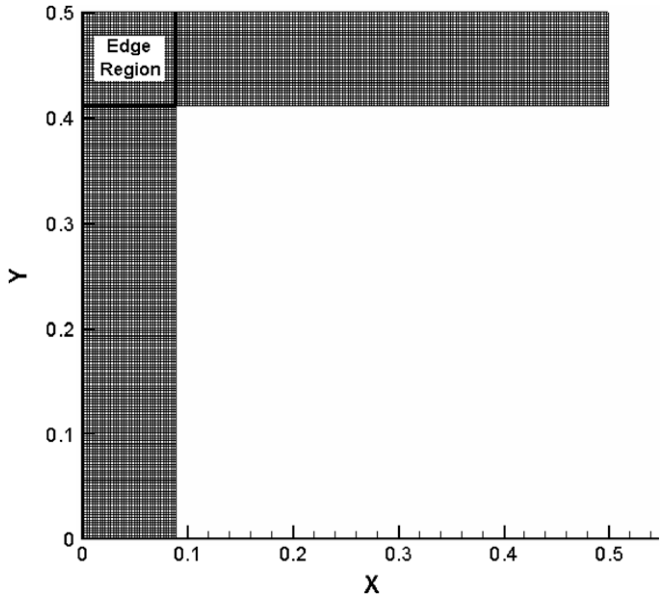

Fig. 1. Corner dimensions (in m) and the regular Cartesian mesh used in the simulations.

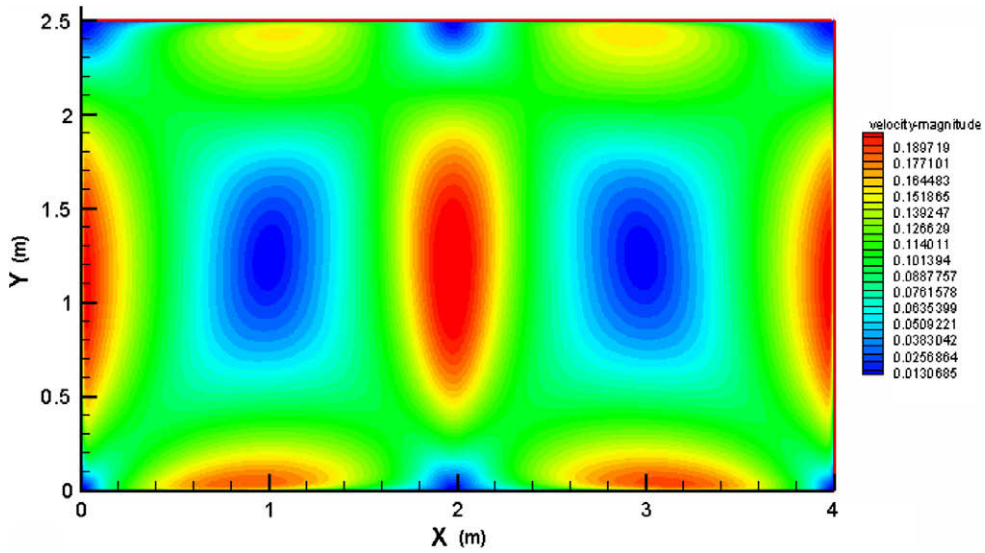

Fig. 2. Stagnation region observed in the buoyancy case.

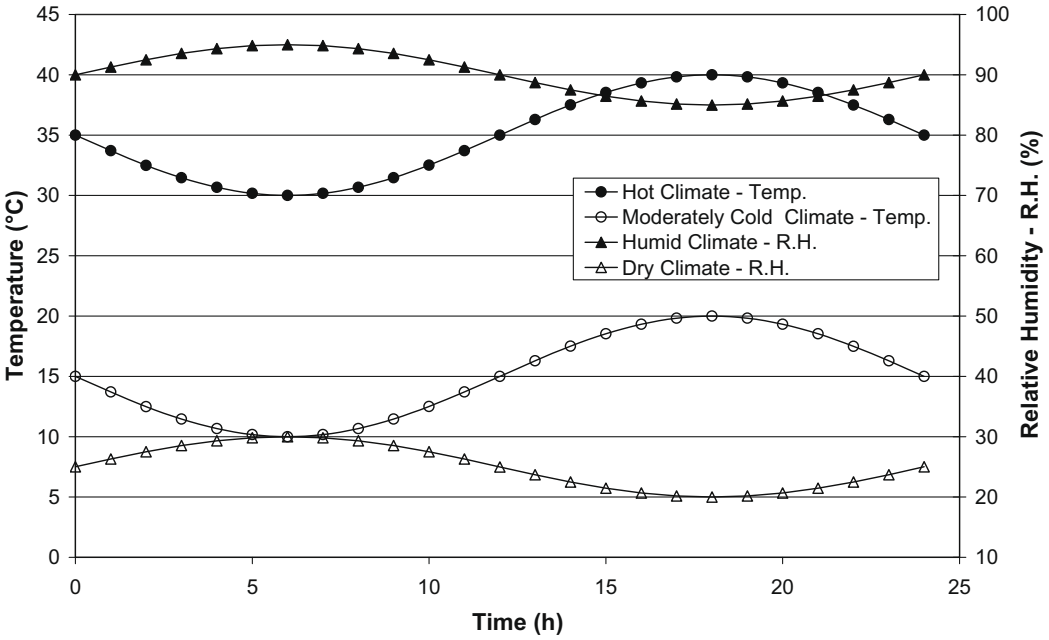

Fig. 3. Temperature and relative humidity variations for hot and moderately cold climates.

$$P_{g,\infty} = P_{g,\mathrm{sup}}. \tag{16}$$

For the moisture flow, vapor transport is considered due to the difference between the partial vapor pressure in air and at the external and internal surfaces:

$$j = \beta_v(p_{v,\infty} - p_{v,\mathrm{sup}}), \tag{17}$$

where j is the density of moisture flow rate (kg/m^2 s) and β_v is the surface coefficient of water vapor transfer (s/m), calculated from the Lewis' relation.

For the heat transport convection heat transfer and phase change were considered:

$$q = h(T_\infty - T_{\mathrm{sup}}) + \beta_v(p_{v,\infty} - p_{v,\mathrm{sup}})L(T), \tag{18}$$

where q is the heat flowing into the structure (W/m^2) and h is the convective heat transfer coefficient (W/m^2 K).

2.5. Solution of the balance equations

A fully-implicit central-difference scheme has been considered for the discretization using the finite-volume method [18]. Implicit schemes demand the use of an algorithm to solve tri-diagonal systems of linear equations. However, for strongly-coupled equations of heat transfer problems, a more robust algorithm is needed in order to achieve numerical stability.

In this way, the MTDMA (MultiTriDiagonal-Matrix Algorithm) has been utilized for solving the balance equations. This algorithm emerged from the need of obtaining all the dependent variable profiles simultaneously at a given time step avoiding numerical

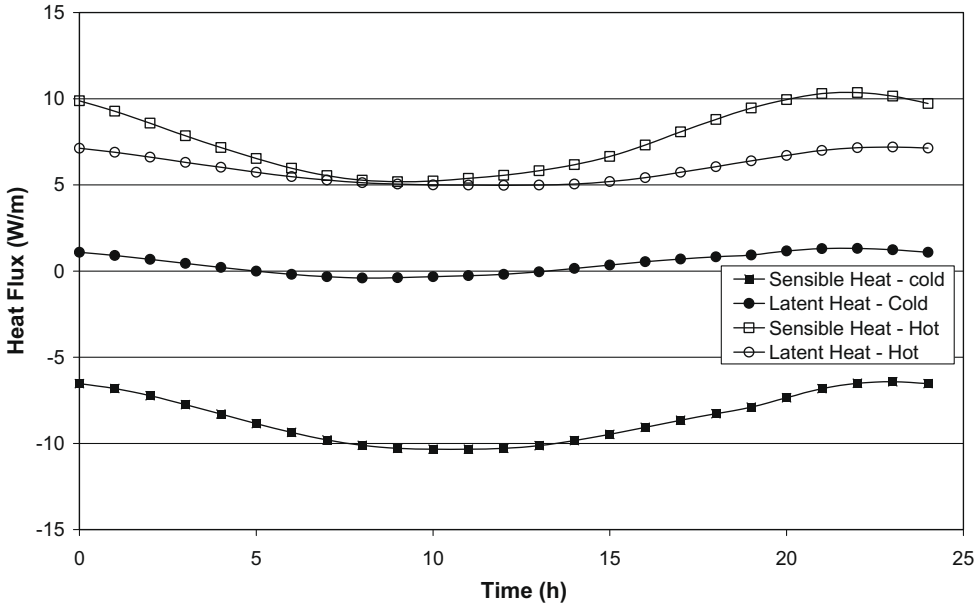

Fig. 4. Effect of the external humidity climate on the corner and edge region of brick.

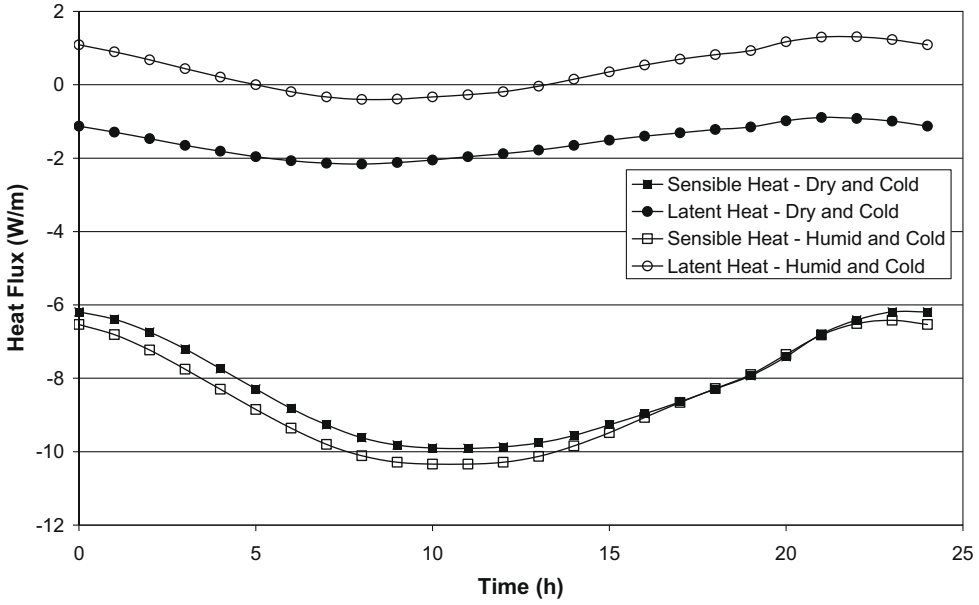

Fig. 5. Sensible and latent thermal load in the cold climate varying the external humidity.

divergence caused by the evaluation of coupled terms from previous iteration values.

3. Simulation procedure

In order to focus on the upper corner, a 0.5-m L-shaped domain (Fig. 1) – divided into 2.5-mm^2 cells of a regular Cartesian mesh – has been considered for all simulations. A 0.09-m thickness brick wall has been used, changing only the edge region (9 cm^2) material from brick to concrete and to insulation. The hygrothermal properties have been obtained from the benchmark of the European project HAMSTAD [19], which has also been used for verification of a 1-D model version. Related works showing other applications using a derived version for one-dimensional and hollow block models have been presented in [20,21].

Externally the corner, a constant uniform value of 10 W/m^2 K has been considered for the convective heat transfer coefficient. Internally, two regions have been defined due to the high differences of air velocity. First, a stagnation region has been defined by means of fluid dynamics simulation utilizing a commercial CFD package FLUENT [22]. In those simulations, the two-dimensional domain has been considered as a 4-m-width-per-2.5-m-height rectangle. The envelope has been considered isothermal and different configurations of hot and cold walls have been analyzed, using the well-known low Reynolds number k–ε turbulence model as proposed by Potter and Underwood [23]. Considering all the configurations, a stagnation region has been noticed within from 20 to 30 cm from the upper internal vertex. As the simulations are recognized to be rather qualitative than quantitative due to many uncertainties presented in the airflow patterns inside

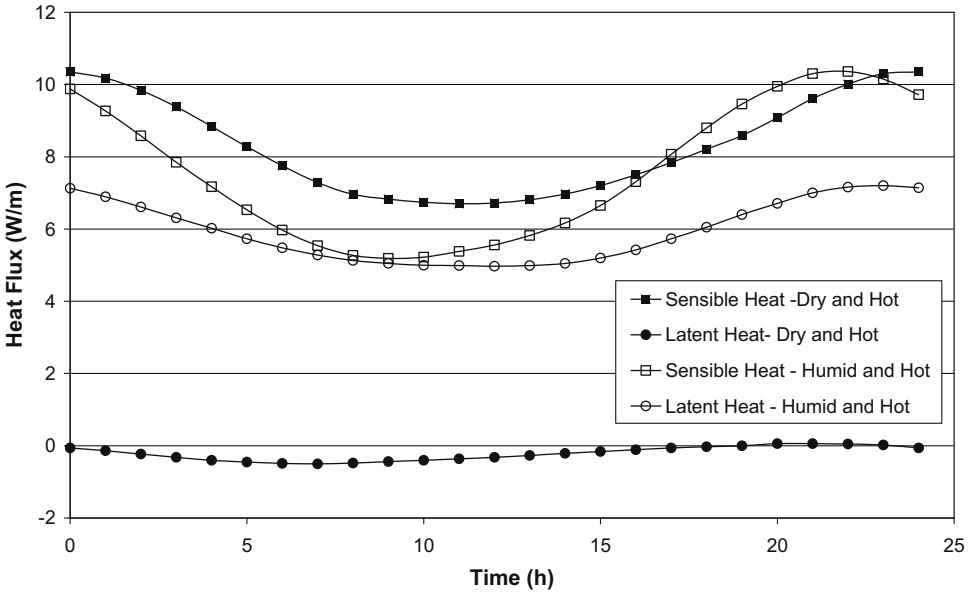

Fig. 6. Sensible and latent thermal load in the hot climate varying the external humidity.

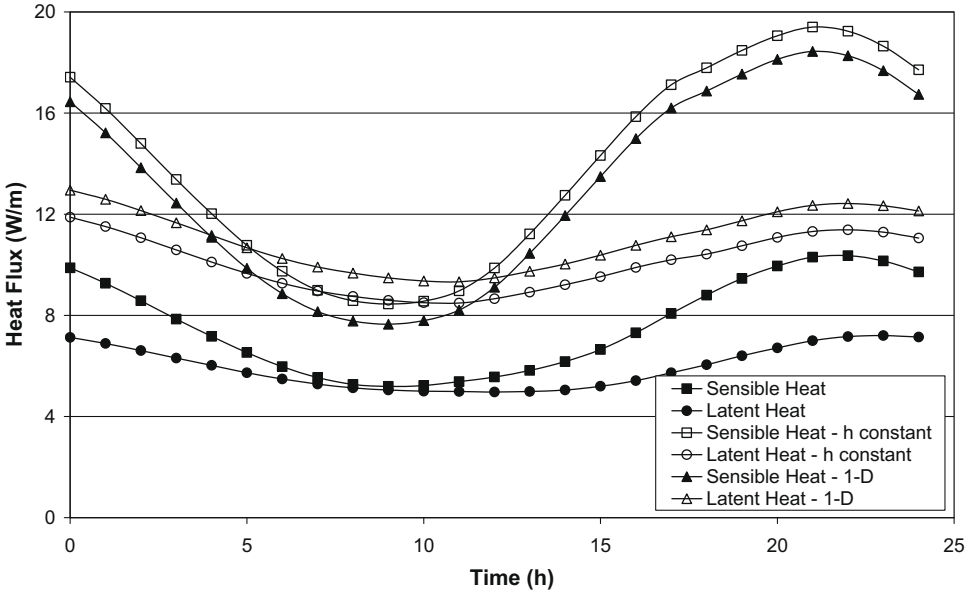

Fig. 7. Sensible and latent thermal load considering uniform and non-uniform internal convective heat transfer coefficients.

a building room, a conservative 20-cm distance from the internal vertex on both axes has been considered as the stagnation region in order to predict the hygrothermal performance and the mould growth risk. In this region, the heat flux occurs predominantly by conduction and a heat flux equivalent resistance has been calculated so that a 0.1-W/m^2 K convective heat transfer coefficient has been considered; outside the stagnant region, a constant 3-W/m^2 K value has been used.

Fig. 2 shows a 48,048-volume steady-state simulated case, where the lower horizontal wall has been kept at 298 K, while the others at 293 K. In that case, the velocity profile shows that the stagnation region could be defined as a 30-cm square from the upper vertex. Those simulations have been only accomplished to estimate a stagnation region. For analyzing the convective phenomenon in a more profound way, turbulence models, wall function and mesh refinement should be examined more rigorously.

As boundary conditions, the internal surfaces have been exposed to air at 24 °C and 50% or 80% of relative humidity. At the external side, sinusoidal variations of temperature and relative humidity during the day have been taken into account. Fig. 3 shows the temperature and relative humidity variations for hot and moderately cold climates.

In order to reduce the initial condition effects, all results presented refer to the 31st day of the simulation.

4. Results

In the analysis hygrothermal of the corner, the Fig. 4 illustrates the effect of the external climate in this region. In Figs. 4–8, the internal surfaces of the corner have been exposed to air at 24 °C and 50% of relative humidity. The external surfaces (Fig. 4) have

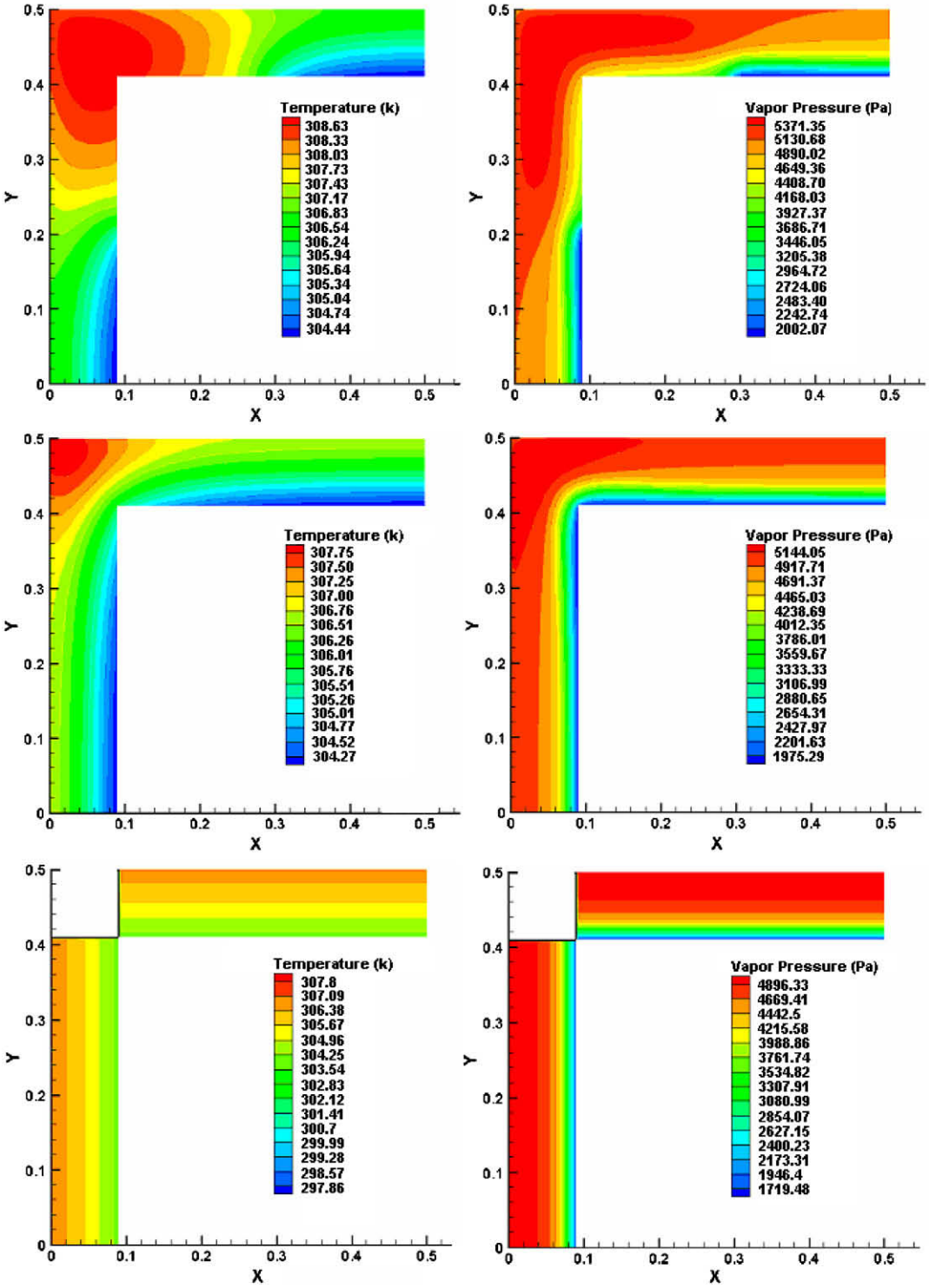

Fig. 8. Corner with non-uniform (top), uniform (intermediary) internal convective heat coefficients and without edge region (bottom) at 12 pm submitted to a humid and hot external climate.

been submitted to humid (cold and hot) climates. The heat fluxes presented in all figures were integrated over the internal corner surface shown in Fig. 1. A significant effect of sensible heat flux is observed in both cases. For the hot climate conditions, the latent heat had higher influence than the one for cold climate conditions, as one could expect.

In Figs. 5 and 6, the humidity effect on the heat flux has been analyzed for cold and hot climates, respectively. The influence of the cold climate (Fig. 5) on the partial vapor pressure at the internal corner surface is smaller than the one for the hot climate (Fig. 6). In the dry and hot climate, the thermal load is basically attributed to sensible heat, while in the humidity and hot climate is observed the great effect of latent heat on the thermal load.

Fig. 7 shows the influence of the internal convective heat transfer coefficient on the heat flux at the corner. Although the average temperature and vapor pressure are lower in the uniform convec-

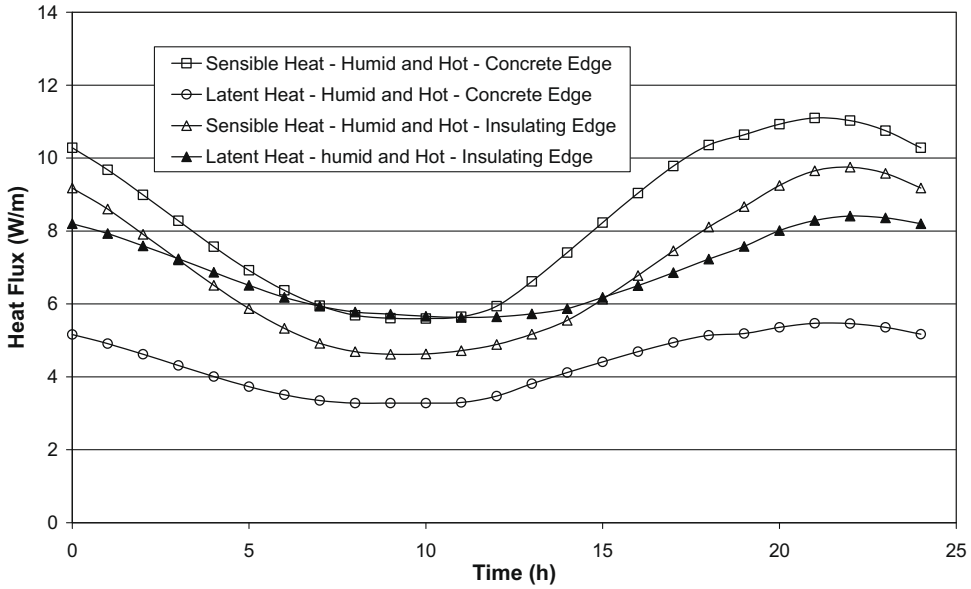

Fig. 9. Comparison between the sensible and latent heat fluxes at the corner with concrete and insulating materials for the edge region.

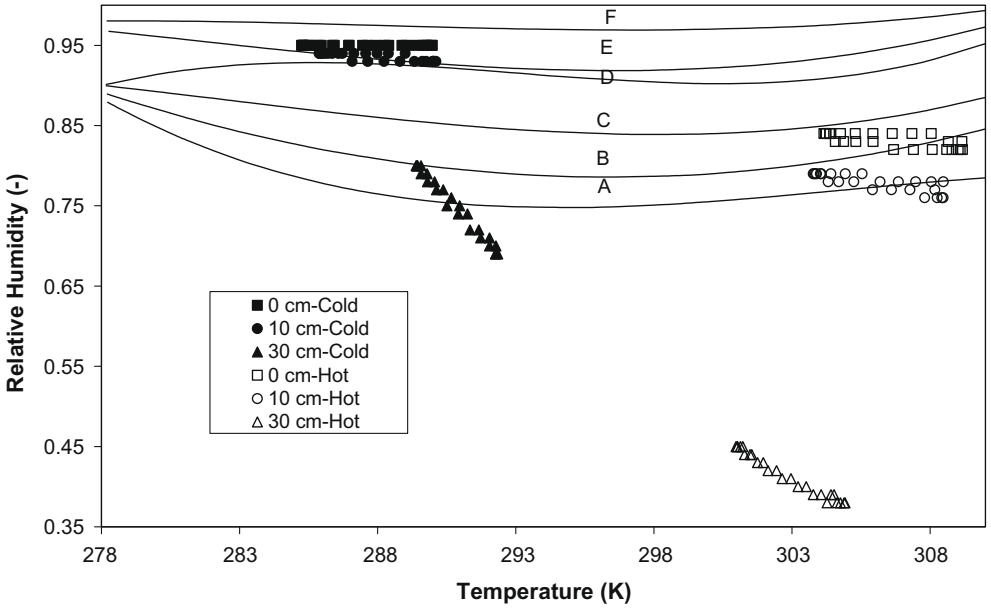

Fig. 10. Prediction of mould growth within the corner region (brick edge).

tive heat transfer coefficient case (Fig. 8), the stagnation region causes a decrement on the sensible and latent thermal load due to the low convective heat and mass transfer coefficients. It has been observed in Fig. 7 that heat flux values obtained from the one-dimensional model (without edge region) agrees well with the one obtained from the two-dimensional model using a uniform internal convective heat transfer coefficient. The difference between the results can be attributed to the multidimensional effect of the edge region (Fig. 8), more sensitive to outdoor climate variations. However, when the phenomena of both stagnation and multidimensionality are compared, the effect of the stagnation region on the heat flux of the corner is predominant.

A comparison between the sensible and latent heat fluxes in the concrete and insulating junctions is illustrated in Fig. 9. The insulating configuration has been proposed for reducing thermal effects through the edge region. The humid and hot external climate has been considered, while the corner internal surfaces have been exposed to air at 24 °C and 80% of relative humidity. As verified in Fig. 9, the sensible heat flux was smaller through insulation junction as expected. However, due to the high hygroscopicity, the latent heat flux through the insulation junction was higher than the one calculated for the concrete junction, causing a higher total heat flux.

In the growth mold risk analysis, the model proposed by Clarke et al. [13] was utilized. In this model, the classes (A, B, C, D, E and F) represent different moisture limits of mould fungi, from highly xerophilic (*chersophilous*) up to highly hydrophilic (moisture-loving). Representatives of those classes are for example *Aspergillus repens* (highly xerophilic), *Aspergillus versicolor* (xerophilic), *Penicillium chrysogenum* (moderately xerophilic), *Cladosporium sphaerospermum* (moderately hydrophilic), *Ulocladium consortiale* (hydrophilic) and *Stachybotrys atra* (highly hydrophilic).

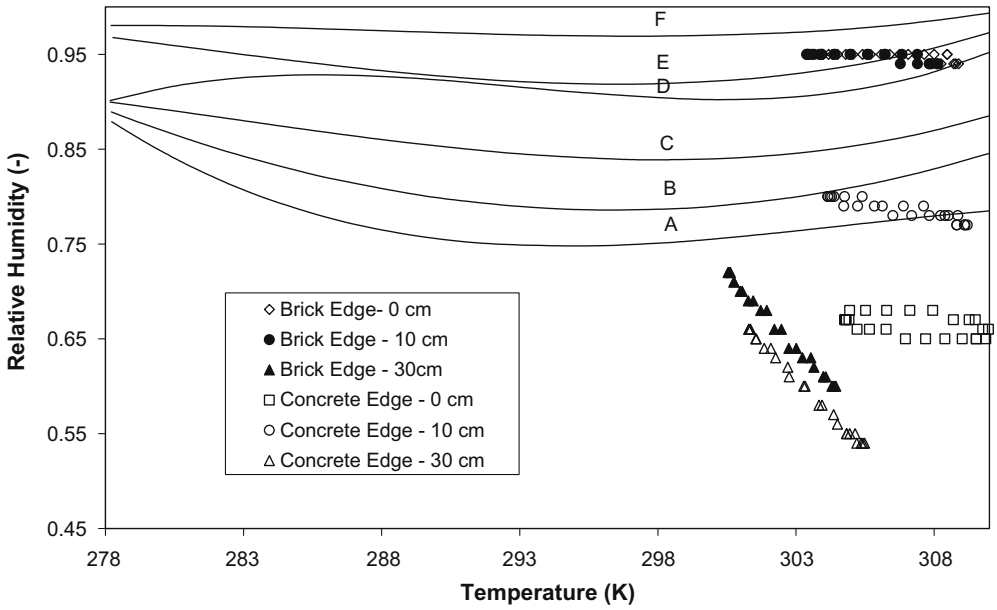

Fig. 11. Prediction of mould growth within the corner region for different materials in the edge region.

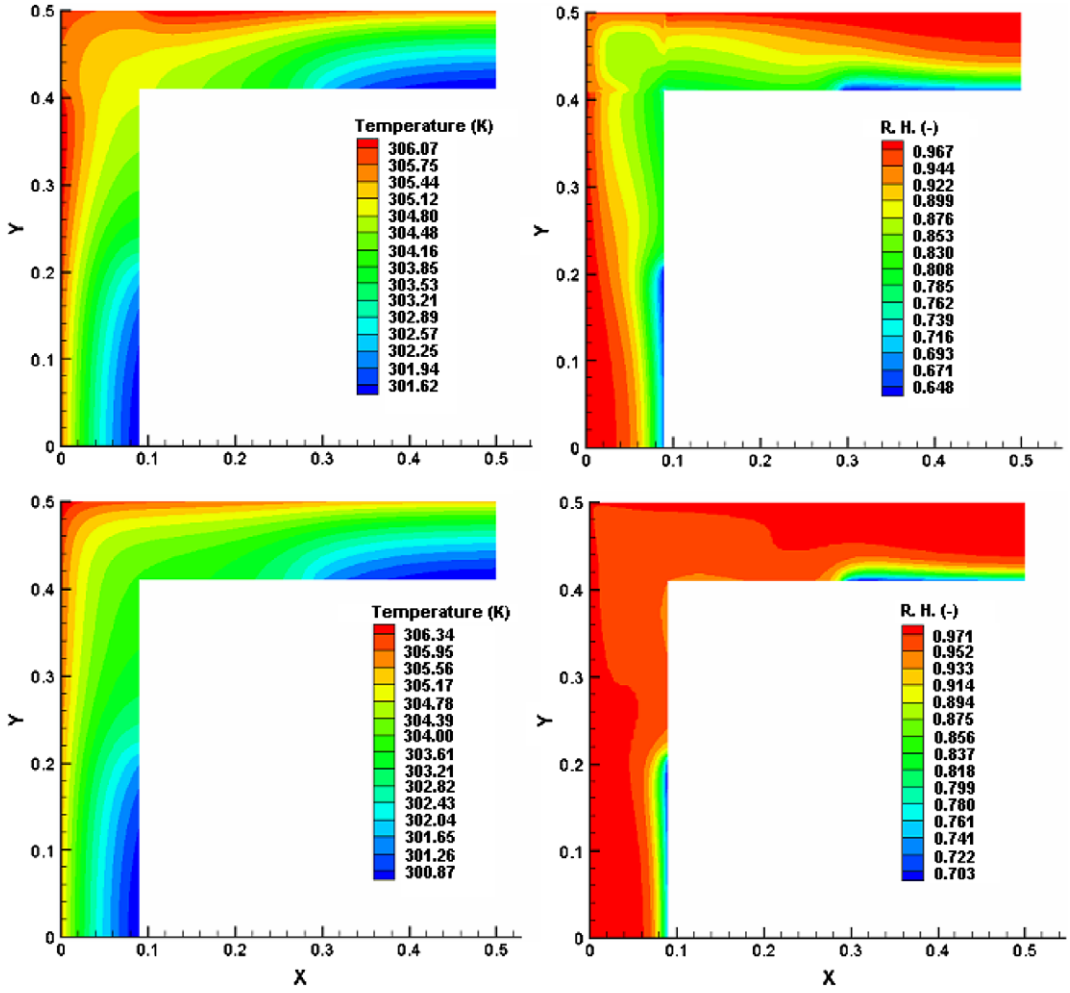

Fig. 12. Concrete (upper figures) and brick (lower figures) edge regions at 12 am.

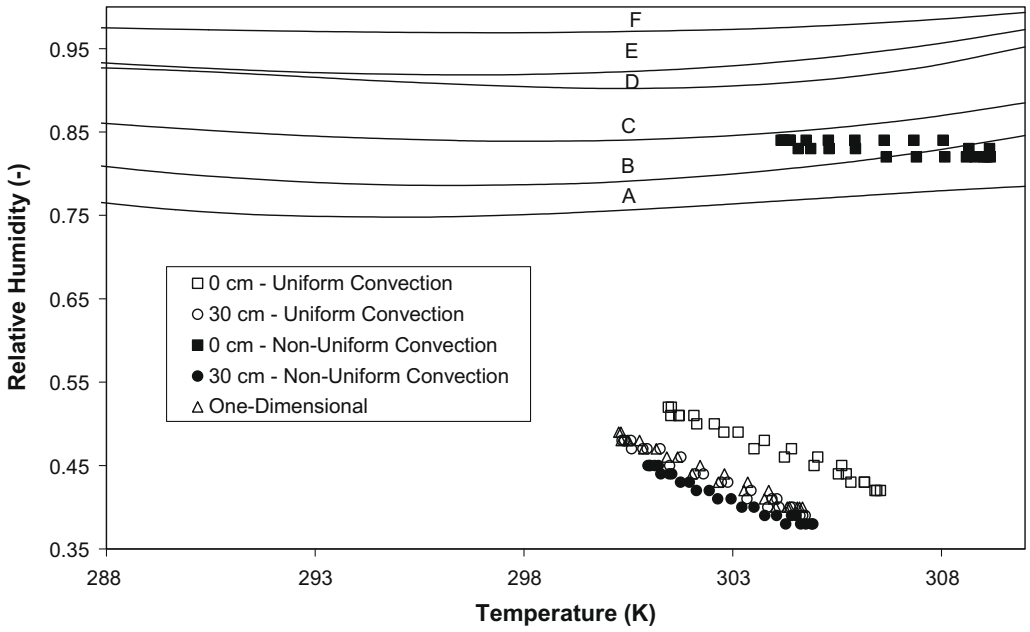

Fig. 13. Convective and multidimensional effect analysis in the mould growth.

In Fig. 10, hourly temperature and relative humidity for three points are plotted: at the internal vertex, 10 cm from internal vertex and 30 cm from internal vertex. The internal surfaces of the upper corner have been exposed to air at 24 °C and 50% of relative humidity. The external surfaces have been submitted to the humid (hot and cold) climates.

For the moderately cold climate, the majority of points are located within the mould growth region. In this case, the relative humidity of the internal surface tends to be higher than that obtained for a hot climate. A moisture concentration close to the internal vertex is observed in both cases due to air stagnation.

In Fig. 11 the effect of the concrete edge is shown. The internal surfaces of the corner have been exposed to air at 24 °C and 80% of relative humidity. The external surfaces have been submitted to a hot and humid climate. In the region near the internal vertex, the relative humidity within the concrete edge was lower than the one calculated within the brick material, reducing the growth mould probability, as observed in Fig. 12. This fact is attributed to the higher hygrothermal capacity of the concrete in comparison to the brick.

In Fig. 13, the convective and multidimensional corner effects are analyzed. The same boundary conditions used to generate results presented in Fig. 10 have been used, however, for the uniform convection condition, an average value of 3 W/m^2 K has been considered for all the control-volume surfaces in contact with indoor air. It has been observed in Fig. 13 only the case in which the stagnation region is considered, the mould growth region is reached. The convective effect is observed clearly in Fig. 8 by means of the temperature and vapor pressure profiles. Therefore, only in the stagnation region, appropriate conditions of temperature and relative humidity are reached for growing mould. This fact shows that mould growth prediction can be misestimated if a simplified one-dimensional building envelope model or a uniform convective heat transfer coefficient is used.

5. Conclusions

A combined building corner multidimensional heat, air and moisture transfer model has been presented for analysis of phenomena such as building hygrothermal performance and mould growth risk. The equations have been discretized using a finite-volume fully-implicit method and then solved by means of the MTDMA (MultiTriDiagonal-Matrix Algorithm), calculating simultaneously at each iteration level the spatial distribution of temperature, partial vapor pressure and moist air pressure. The chosen algorithm provides much more stability due to the fact the three governing equations are strongly interdependent.

Results have been presented for the purposes of analyzing both hygrothermal performance and mould growth risk around the corner internal vertex. Expectedly, the edge regions have shown to be more sensitive to outdoor climate variations, even under constant external and internal convective heat transfer coefficients. In the case of no-constant coefficients (air stagnation region), the multidimensional effect becomes more evident. This fact shows that in programs where a simplified one-dimensional model is used for the building envelope, the thermal load and mould growth estimations may generate serious errors due to corner effects.

The corner hygrothermal analysis has shown the great latent heat effect on the total thermal load, mainly under a hot and humid external climate. Additionally, it has been observed that mould growths predominantly in the corner region due especially to the low convective effect noticed within the stagnation region. In this region, an increase of the relative humidity is promoted making easier the mould growth, mainly when a cold and humid external climate is considered.

Acknowledgments

The authors thank CNPq – Conselho Nacional de Desenvolvimento Científico e Tecnológico – of the Secretary for Science and Technology of Brazil and Araucária Foundation for support of this work.

References

[1] BEN – Balanço Energético Nacional 2007: Ano base 2006, Ministério de Minas e Energia, Relatório Final, 2007.
[2] D. Crawley, J.W. Hand, M. Kummert, B.T. Griffith, Contrasting the Capabilities of Building Energy Performance Simulation Programs, Report of the United States Department of Energy, 2005.

[3] W.P. Brown, A.G. Wilson, CBD-44, Thermal Bridges in Buildings, 1963. Available from: <http://irc.nrc-cnrc.gc.ca/pubs/cbd/cbd044_e.html>.
[4] S. Hassid, Thermal bridges across multilayer walls: an integral approach, Build. Environ. 25 (1990) 143–150.
[5] S. Hassid, Algorithms for multi-dimensional heat transfer in buildings, in: International IBPSA Conference, 1991, pp. 9–13.
[6] M. Krarti, Heat loss and moisture condensation for wall corners, Energy Convers. Manage. 35 (8) (1994) 651–659.
[7] D. Tang, G.S. Saluja, Analytic analysis of heat loss from corners of buildings, Int. J. Heat Mass Transfer 41 (4–5) (1998) 681–689.
[8] S. Farkh, Ponts Thermiques, Th-U, Fascicule 5/5, 2001, 133 p.
[9] L. Olsen, N. Radisch, Thermal Bridges in Residential Buildings in Denmark, Danish Technological Institute, ISBN – 80-902689-6-X, 2002, 19 p.
[10] T. Csoknyai, Surface temperature a thermal bridges, J. Build. Phys. 25 (67) (2001).
[11] J. Kosny, E. Kossecka, Multi-dimensional heat transfer through complex building envelope assemblies in hourly energy simulation programs, Energy Build. 34 (2002) 445–454.
[12] O. Adan, On the Fungal Defacement of Interior Finishes, Dissertation, University of Technology, Eindhoven, 1994.
[13] J.A. Clarke et al., A technique for the prediction of the conditions leading to mould growth in buildings, Build. Environ. 34 (1999) 515–521.
[14] A. Hukka, H.A. Viitanen, A mathematical model of mould growth on wooden material, Wood Sci. Technol. 33 (1999) 457–485.
[15] H.J. Moon, G. Augenbroe, Evaluation of hygrothermal models for mold growth avoidance prediction, in: Eighth International IBPSA Conference, 2003, pp. 895–902.
[16] N. Mendes, P.C. Philippi, R.A. Lamberts, New mathematical method to solve highly coupled equations of heat and mass transfer in porous media, Int. J. Heat Mass Transfer 45 (2002) 509–518.
[17] N. Mendes, P.C. Philippi, A method for predicting heat and moisture transfer through multilayered walls based on temperature and content gradients, Int. J. Heat Mass Transfer 48 (2005) 37–51.
[18] S.V. Patankar, Numerical Heat Transfer and Fluid Flow, Hemisphere Publishing Corporation, 1980.
[19] C.E. Hagentoft, HAMSTAD – WP2 Modeling, Report R-02:9, Gothenburg, Department of Building Physics, Chalmers University of Technology, 2002.
[20] G.H. Santos, N. MENDES, Combined heat, air and moisture (HAM) transfer model for porous building materials, J. Build. Phys. 32 (2009) 203–220.
[21] G.H. Santos, N. Mendes, Heat, air and moisture transfer through hollow porous blocks, Int. J. Heat Mass Transfer 52 (2009) 2390–2398.
[22] FLUENT, Release 6.3, Users's Guide, 2006.
[23] S.E. Potter, C.P. Underwood, A modelling method for conjugate heat transfer and fluid flow in building spaces, Build. Serv. Eng. Res. Technol. 25 (2) (2004) 111–125.